Annals of Biomedical Engineering, Vol. 37, No. 11, November 2009 (© 2009) pp. 2170–2187
DOI: 10.1007/s10439-009-9764-4

New Cardiac MRI Gating Method Using Event-Synchronous Adaptive Digital Filter

HODONG PARK,[1,4] YOUNGCHEOL PARK,[2] SUNGPIL CHO,[1] BONGRYOEL JANG,[3] and KYOUNGJOUNG LEE[1]

[1]Department of Biomedical Engineering, College of Health Science, Yonsei University, 234, Maeji-Ri, Heungup-Myon, Wonju City, Kangwon Do 220-710, Korea; [2]Department of Computer & Telecomm Engineering, Yonsei University, Wonju City, Korea; [3]AILab Co, Wonju City, Korea; and [4]Research and Development Team, MEZOO Co, 1272, Maeji-Ri, Heungup-Myon, Wonju City, Kangwon Do 220-710, Korea

(*Received 13 December 2007; accepted 21 July 2009; published online 31 July 2009*)

Abstract—When imaging the heart using MRI, an artefact-free electrocardiograph (ECG) signal is not only important for monitoring the patient's heart activity but also essential for cardiac gating to reduce noise in MR images induced by moving organs. The fundamental problem in conventional ECG is the distortion induced by electromagnetic interference. Here, we propose an adaptive algorithm for the suppression of MR gradient artefacts (MRGAs) in ECG leads of a cardiac MRI gating system. We have modeled MRGAs by assuming a source of strong pulses used for dephasing the MR signal. The modeled MRGAs are rectangular pulse-like signals. We used an event-synchronous adaptive digital filter whose reference signal is synchronous to the gradient peaks of MRI. The event detection processor for the event-synchronous adaptive digital filter was implemented using the phase space method—a sort of topology mapping method—and least-squares acceleration filter. For evaluating the efficiency of the proposed method, the filter was tested using simulation and actual data. The proposed method requires a simple experimental setup that does not require extra hardware connections to obtain the reference signals of adaptive digital filter. The proposed algorithm was more effective than the multichannel approach.

Keywords—ECG, MR gradient artefacts, Cardiac gating, Event synchronous, Adaptive digital filter.

INTRODUCTION

Magnetic resonance imaging (MRI) is a clinically important medical imaging modality, and it provides biomedical, anatomical, and functional information on biochemical compounds within any cross section of the human body.

When imaging the heart using MRI, a clean and artefact-free electrocardiograph (ECG) signal is not only important for monitoring the patient's heart activity and heart rate but also essential for cardiac gating. Because conventional MRI images are formed from a number of sequence repetitions, imaging a moving organ, such as the heart, requires each sequence to be triggered at the same part of the cardiac cycle. Several different triggering techniques can be used, including finger plethysmography and carotid pulse tracings, but ECG is the most widely used technique.[15]

ECG gating using a cardiac cycle can synchronize MRI sequence acquisition to an ECG R-wave in order to eliminate image motion artefacts induced by heart and vessel contractions, as well as pulsatile flow in the blood vessels. A fundamental problem associated with using conventional ECG to monitor a subject's cardiac activity during performing MRI is ECG distortion induced by electromagnetic interference. ECG signals are heavily disturbed by static magnetic field interference and magnetic-gradient-related interference. In addition, distortion of the ECG trace due to time-varying gradients can be very large and unpredictable for some combinations of the patient anatomy, sequence type, electrode placement, and quality of contact.

Furthermore, all of these examples produce artefacts that may vary from one individual to another, as well as on a beat-to-beat basis within the same individual. A possible method for the removal of artefacts would be suppression using numerical techniques, because the artefacts are supposedly caused by physiological effects which are caused by time-varying magnetic fields to acquire MRI images.

One of typical physiological effects is the electric field induction. In detail, a steady electric field produces surface charges on conducting objects, including the human body. Positive charges are accumulated on the side of conducting body nearest to the negative

Address correspondence to Kyoungjoung Lee, Department of Biomedical Engineering, College of Health Science, Yonsei University, 234, Maeji-Ri, Heungup-Myon, Wonju City, Kangwon Do 220-710, Korea. Electronic mail: hodong_park@hanmail.net, young00@yonsei.ac.kr, saylas@hanmail.net, brjang@gmail.com, lkj5809@yonsei.ac.kr

source of the field, and negative charges on the side nearest to the positive source. If the field is alternating, the positive and negative charges alternate in position, resulting in an alternating current within the biological medium.

In the past, various strategies have been proposed to enable ECG recording in MR environments.[5,6,12,16–18,21,22] Many published ECG acquisition schemes are based on reduced bandwidths. Further, solutions based on vector cardiograms and MR imaging techniques have been proposed.[8,14] Unfortunately, these solutions are not applicable to patient monitoring. Other MRI artefact suppression methods have been developed for processing MRI signals disturbed during MRI examinations, but most of these methods focus on the ECG for functional MRI (fMRI) applications and often use a predefined MR image sequence.[3,4,7,10,19]

These methods based on fixed filters have certain drawbacks. When a strong magnetic field is radiated by gradient coils, the MR gradient artefacts (MRGAs) induced on the ECG trace depend on the gradient scenarios. Further, the shape of the artefacts induced in the ECG depends strongly on the MRI scan parameters. Therefore, these MRGAs could not be removed by conventional FIR or IIR filters with fixed coefficients. In this case, the filters should be able to adapt to the MRI scan parameters in the ECG trace. To this end, an adaptive filtering technique can be used. The use of an adaptive filter can provide both flexibility and effectiveness. An adaptive filter can be used in any situation where noise interference is embedded in the signal of interest, such as that in the case of field measurements of biological signals.

Recently, combined wavelet sub-band decomposition and adaptive filtering, which are used for the real-time suppression of artefacts caused by MR gradients, have been proposed[2] and the method of suppressing MRGAs using an adaptive noise canceller (ANC) was suggested.[1] The method in Abacherli *et al.*[1] requires gradient pulse signals (G_x, G_y, and G_z) as the reference signals, which are obtained from the MR scanner's gradient amplifier. It has a disadvantage which requires extra hardware connections to obtain the reference signals of adaptive digital filter. The method in Abi-Abdallah *et al.*[2] used a signal processing algorithm based on an adaptive digital filter and a wavelet-based filter bank decomposition strategy that allows the extraction of an efficient reference signal from a contaminated ECG, mainly for MRI synchronization. However this method requires off-line filter computation phase. In the proposed method, the adaptive filter and event detector are computed on-line.

In the study, we proposed an adaptive algorithm for the suppression of MRGAs in the ECG leads of a cardiac MRI gating system. The proposed algorithm uses an event-synchronous adaptive digital filter whose reference signal is synchronous to the gradient peaks of MRI. The main feature of the proposed algorithm is that it extracts the gradient pulses directly from the three-lead ECG signal contaminated by the MRGAs. Therefore, unlike the previous ANC-based method,[1] no external devices are required for acquiring the gradient pulse signals. Instead, the gradient pulses are generated based on a combination of three noisy ECG signals.

The proposed method is independent of the MR scanner such that the real-time system can be constructed with minimum hardware connections. Another advantage of the proposed system is that due to the nature of the synthesized gradient pulses, its adaptation needs to be performed only for the period of the event pulses, which simplifies the algorithm for implementation but robust to the strong ECG component in the desired channel.

The section "Methodology" provides a detailed description of the modeling and suppression of MRGAs using the proposed method. The section "Experimental setup" provides the experiment details and performance metric for the suppression of MRGAs. The section "Results" provides the simulation examples as well as the results of artefact cancellation in order to further understand the improvement in the MR image using the proposed cardiac gating method. Finally, sections "Discussion" and "Conclusion" provide the discussions and conclusions.

METHODOLOGY

Modeling of MRGAs

The origin of interference due to gradient switching is not yet clear; the acquisition wires and/or the tissues of the subject can form an inductive loop. Therefore, we have modeled MRGAs as the source of strong pulses that were used for dephasing the MR signal.

The voltages induced by the MR gradient produce artefacts that are added to the electrophysiological signal. A simplified model of MRGA generation is shown in Fig. 1.

The MRGAs included in lead j as a result of varying the MR gradient, denoted by $\alpha_j(t)$, are modeled as follows[1]:

$$\alpha_j(t) = g\left(\vec{B}(t)\right) = -\frac{d\left(\left(\vec{G}(t)\cdot\vec{r}(t)\right)\cdot A(t)\right)}{dt} \quad (1)$$

where $\vec{B}(t)$ is the magnetic field in the MR bore, $\vec{G}(t)$ is a vector containing three gradient signals $G_x(t)$, $G_y(t)$, and $G_z(t)$, $\vec{r}(t)$ are the coordinates of the MR bore where induction of $\vec{B}(t)$ into the human subject occurs, and $A(t)$ is the active area where the magnetic flux

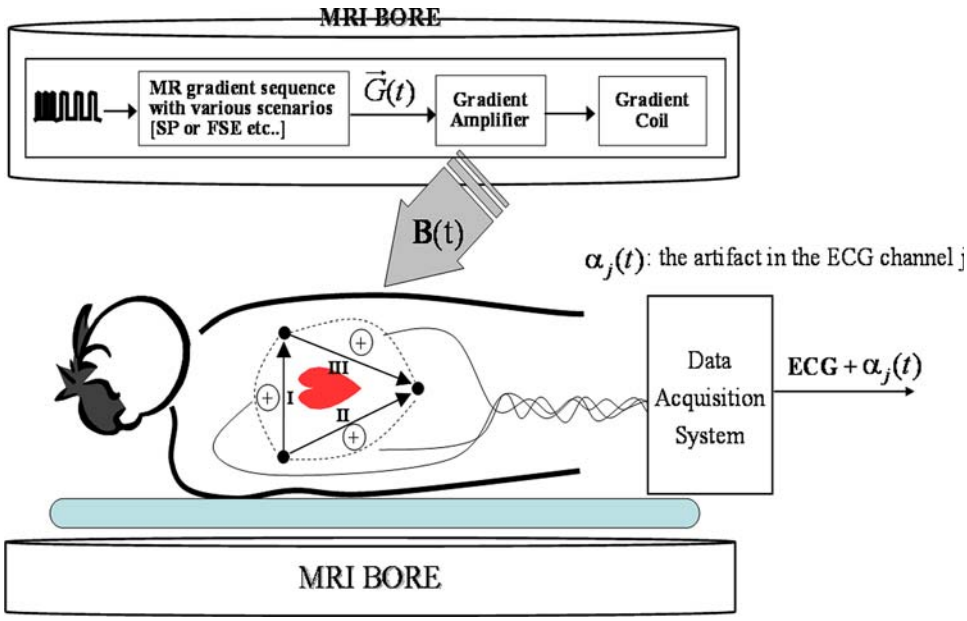

FIGURE 1. Simplified model for MRGA generation.

flows through the human tissue, lead wires, and ECG electrodes. Therefore, if the magnetic field $\vec{B}(t)$ is known, the MRGA in the ECG lead j $\alpha_j(t)$ can be modeled using Eq. (1). However, $\vec{B}(t)$ cannot be detected in practical systems.

From Eq. (1), the MRGA $\alpha_j(t)$ can also be expressed as a function of the gradient vector:

$$\alpha_j(t) = f_{x,j}(G_x(t)) + f_{y,j}(G_y(t)) + f_{z,j}(G_z(t)) \quad (2)$$

where $G_x(t)$, $G_y(t)$, and $G_z(t)$ are the components of $\vec{G}(t)$ along the x, y, and z axis. $f_{k,j}(\cdot)$, $k = x, y, z$ in Eq. (2) denote the functions mapping the x, y, and z gradient components onto $\alpha_j(t)$, and these can be conveniently modeled using linear FIR filters. Thus, we have

$$f_{k,j}(G_k(t)) = \phi_{k,j}(t) \otimes G_k(t), \quad k = x, y, z, \quad (3)$$

where $\phi_{k,j}(t)$ is the impulse response of the path between the gradient components to the MRGA in the ECG lead $\alpha_j(t)$ and $\otimes$ denotes the convolution operation.

Using Eq. (3), Eq. (2) can be rewritten as

$$\alpha_j(t) = \phi_{x,j}(t) \otimes G_x(t) + \phi_{y,j}(t) \otimes G_y(t) + \phi_{z,j}(t) \otimes G_z(t) \quad (4)$$

Therefore, if the gradient components $G_x(t)$, $G_y(t)$, and $G_z(t)$ are known, it is possible to linearly estimate and reduce the artefacts in $\alpha_j(t)$. However, to conform to this assumption, we have to use extra channels to detect the x, y, and z gradient components of the MR, because these components are not generally available.

The gradient components $G_x(t)$, $G_y(t)$, and $G_z(t)$ are dependent on the MR gradient sequence. The MR gradient sequence along each axis comprise gradient selection (GXS), gradient reading (GXR), gradient coding (GXC), and gradient coding static (GXCS). Further, the sequence of $G_x(t)$, $G_y(t)$, and $G_z(t)$ required for switching three gradient amplifiers generally comprises a rectangular-like pulse. Each sequence of the three gradient components is synchronized with a very short time delay. Based on the abovementioned facts, we can conclude that if the generation of the three gradient components is caused by the same source $\sigma(t)$, then the program sequence of the three gradient components can be modeled using $\sigma(t)$.

Thus, the process between the program sequence denoted by $\sigma(t)$ and the gradient components can also be conveniently modeled using linear FIR filters as shown by

$$G_k(t) = \beta_k(t) \otimes \sigma(t), \quad k = x, y, z \quad (5)$$

where $\beta_k(t)$ is the impulse response of the system between the gradient source $\sigma(t)$ and the x, y, and z components of the gradients $G_x(t)$, $G_y(t)$, and $G_z(t)$. Although the hardware components used in Abacherli *et al.*[1] included nonlinear components, linear modeling of the process is sufficient to estimate MRGAs induced in the ECG lead, which will be confirmed through experiments.

Now, Eqs. (4) and (5) can be rewritten as

$$\alpha_j(t) = \phi_{x,j}(t) \otimes \beta_x(t) \otimes \sigma(t) + \phi_{y,j}(t) \otimes \beta_y(t) \otimes \sigma(t) + \phi_{z,j}(t) \otimes \beta_z(t) \otimes \sigma(t) = \gamma_j(t) \otimes \sigma(t) \quad (6)$$

where

$$\gamma_j(t) = \theta_{x,j}(t) \otimes \beta_x(t) + \theta_{y,j}(t) \otimes \beta_y(t) + \theta_{z,j}(t) \otimes \beta_z(t) \tag{7}$$

Here, $\gamma_j(t)$ denotes a combined impulse response of the possible paths between the gradient source and the ECG lead j.

If the MRGA is extended to the three-lead ECG system, the artefacts induced in Leads I, II, and III ($\alpha_{\mathrm{I}}(t)$, $\alpha_{\mathrm{II}}(t)$, and $\alpha_{\mathrm{III}}(t)$) can be expressed as

$$\alpha_j(t) \cong \gamma_j(t) \otimes \sigma(t), \quad j = \mathrm{I}, \mathrm{II}, \mathrm{III} \tag{8}$$

Thus, given a gradient source $\sigma(t)$, $\gamma_j(t)$ can be estimated using the model in Eq. (8). However, *a priori* information about $\sigma(t)$ is generally not available unless $\sigma(t)$ is directly detected from the MRI hardware system. Therefore, we have to develop a method of estimating the gradient source signal. To this end, we utilize the "three-lead vector system" within the ECG because it is necessary to acquire the artefact-only signal induced by the MR gradients.

Suppression of MRGAs

The contaminated ECG signal contains both the ECG signal and MRGAs. The output of the ECG lead j can be expressed as

$$l_j(n) = c_j(n) + a_j(n), \quad j = \mathrm{I}, \mathrm{II}, \mathrm{III} \tag{9}$$

where $c_j(n)$ and $a_j(n)$ are the sampled versions of the pure ECG signal and the MRGA in the ECG lead j. To estimate the MRGA in the ECG leads, the minimum mean-square error (MMSE) criterion can be applied to the models in Eqs. (4) and (6). Figures 2 and 3 show the schematic diagrams of the models described in Eqs. (4) and (6).

Equation (4) and Fig. 2 indicate that given the gradient components, the MRGA in the ECG lead can be linearly modeled using a multichannel filter. Thus, the MRGA in the ECG lead j is estimated as follows[11]:

$$\hat{a}_j(n) = \mathbf{W}_j^T \mathbf{G}(n) \tag{10}$$

where

$$\begin{aligned} \mathbf{W}_j &= \left[\mathbf{w}_{x,j}^T\ \mathbf{w}_{y,j}^T\ \mathbf{w}_{z,j}^T\right]^T, \\ \mathbf{G}(n) &= \left[\mathbf{g}_x^T(n)\ \mathbf{g}_y^T(n)\ \mathbf{g}_z^T(n)\right]^T \end{aligned} \tag{11}$$

and $\mathbf{w}_{x,j}$, $\mathbf{w}_{y,j}$, and $\mathbf{w}_{z,j}$ are the $(N \times 1)$ weight vectors being applied to the x, y, and z gradient inputs contained in the vectors $\mathbf{g}_x(n)$, $\mathbf{g}_y(n)$, and $\mathbf{g}_z(n)$, respectively. The estimation error is formulated as

$$e_j(n) = l_j(n) - \hat{a}_j(n). \tag{12}$$

The optimum weight vectors are obtained by using the MMSE criterion where the mean-square error (MSE) function is defined as $\xi_j = E\left\{|e_j(n)|^2\right\}$. The optimum weight vector is then given by

$$\mathbf{W}_j^o = \mathbf{R}^{-1}\mathbf{p}_j \tag{13}$$

where $\mathbf{R} = E\{\mathbf{G}(n)\mathbf{G}^T(n)\}$ and $\mathbf{p}_j = E\{l_j(n)\mathbf{G}(n)\}$ denote the $(3N \times 3N)$ autocorrelation matrix and $(3N \times 1)$ cross-correlation vector, respectively.

Abacherli *et al.*[1] proposed a method of estimating the MRGAs using an adaptive digital filter. They used three additional analog gradient signals acquired from the gradient coil of the MRI system. This method has some drawbacks, e.g., an additional hardware interface circuit is necessarily required for acquiring the three-axis gradient signals and the system can become complex because the system is dependent on MRI.

On the other hand, using Eq. (6) and Fig. 3, the MRGA in the ECG lead j can also be modeled as

$$\hat{a}_j(n) = \mathbf{h}_j^T \mathbf{s}(n) \tag{14}$$

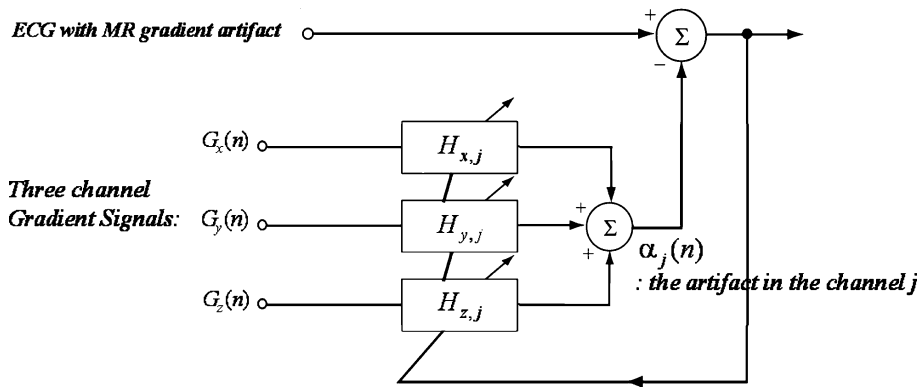

FIGURE 2. Schematic diagram of model to estimate MRGA using three-channel gradient signals. $G_x(n)$, $G_y(n)$, and $G_z(n)$ are analog gradient signals acquired from the gradient coil of the MRI system in the *x*, *y*, and *z* axis. $H_{x,j}$, $H_{y,j}$, and $H_{z,j}$ are weight vectors being applied to the *x*, *y*, and *z* gradient input signals. $\alpha_j(n)$ is the estimated artefact signal in the each three channels.

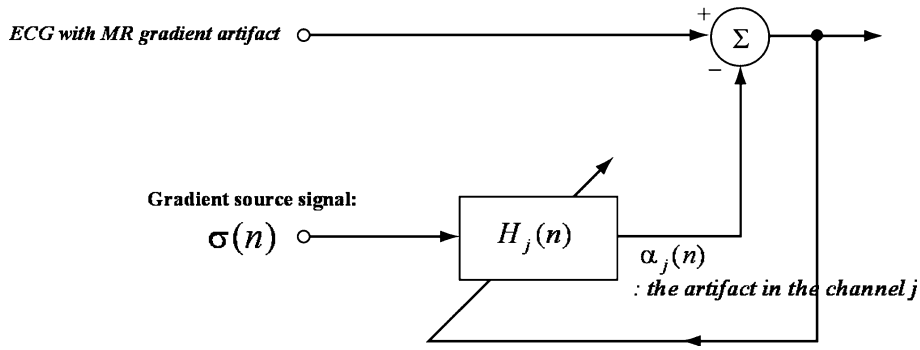

FIGURE 3. Schematic diagram of model to estimate MRGAs using gradient source $\sigma(t)$.

where $\mathbf{h}_j$ and $\mathbf{s}(n)$ are the $(M \times 1)$ weight vector $[h_{j,0}, h_{j,0},\ldots,h_{j,M-1}]^T$ and the reference input vector $[s(n), s(n-1), \ldots, s(n-M+1)]^T$ containing samples of the gradient source signal $\sigma(t)$. Now, the MRGA is modeled using a single-channel filter whose weight vector is determined according to the MMSE criterion as

$$\mathbf{h}_j^o = \mathbf{\Phi}^{-1}\boldsymbol{\theta}_j \tag{15}$$

where $\mathbf{\Phi} = E\{\mathbf{s}(n)\mathbf{s}^T(n)\}$ and $\boldsymbol{\theta}_j = E\{l_j(n)\mathbf{s}(n)\}$ denote the $(M \times M)$ autocorrelation matrix and $(M \times 1)$ cross-correlation vector, respectively.

The main difference between the two approaches in Eqs. (10) and (14) is the input signal to the filters. In the former approach, three gradient signals $\mathbf{g}_x(n)$, $\mathbf{g}_y(n)$, and $\mathbf{g}_z(n)$ are used as the reference inputs to the multichannel filter, which are obtained from the hardware interface, and the sampling rate should be sufficiently high to accurately acquire the gradient shapes; further, greater computational complexity is required for real-time implementation. However, in the latter approach, a single-reference channel is used instead of three reference channels. Thus, the filter required in the second approach has a simpler and more efficient structure than that required in the first approach, only if the gradient source signal $\mathbf{s}(n)$ is available. Like the gradient components, however, the gradient source signal is not available in general. Thus, either an extra hardware interface or a signal processing technique is required for estimating $\mathbf{s}(n)$ from the available signals.

In this paper, we propose a method for synthesizing the reference signal and estimating the gradient source signal from the vector sum of the three contaminated ECG leads. The synthesized reference signal models the MR gradient source signal using unit square pulses which are generated at the positions of the detected peaks to yield the gradient source signal $\sigma(t)$ or $\mathbf{s}(n)$. Thereafter, the generated square pulses are then applied to the estimation filter as the reference input. As a consequence, the proposed algorithm does not require extra hardware connections to obtain the reference signals. Furthermore, the adaptive algorithm for the single-channel model in Eq. (14) becomes much simpler due to the special structure of the reference signal, which will be discussed below.

Synthesis of Gradient Source for Reference Input

The gradient source signal used as the reference signal for the filter shown in Fig. 3 is not available in general.

In the contaminated ECG measurements, a vector sum defined by "Lead I − Lead II + Lead III" yields a characteristic function with a zero value. However, the MRGAs in the three ECG leads are not cancelled by the vector sum. Therefore, the vector sum will include only the artefacts induced by the MR gradients. The remaining artefacts after the vector sum can be considered as signals with arbitrary direction vectors, which are different from the original directions of Leads I, II, and III.

The vector sum produces

$$\begin{aligned}\eta(n) &= l_{\mathrm{I}}(n) - l_{\mathrm{II}}(n) + l_{\mathrm{III}}(n) \\ &= \alpha_{\mathrm{I}}(t) - \alpha_{\mathrm{II}}(t) + \alpha_{\mathrm{III}}(t) + \varepsilon(n)\end{aligned} \tag{16}$$

where $\eta(n)$ is the vector sum of the three leads and $\varepsilon(n)$ is the residue of the ECG component after the vector sum, which is much smaller than the remaining MRGAs, namely, $\alpha_{\mathrm{I}}(n) - \alpha_{\mathrm{II}}(n) + \alpha_{\mathrm{III}}(n)$.

It should be noted that the vector sum signal can be used as the reference input of the adaptive filter because it mainly comprises the MRGA components. However, the vector sum contains noise only within the periods between the MR gradient pulses. Furthermore, the gradient pulses are generally sparse. Thus, a large portion of the vector sum is filled with noise that is independent of the gradient pulses, which in turn degrades the modeling accuracy of the MRGA in the ECG lead. Further, due to the morphological similarity between the MRGA and ECG signals, the ECG components in the desired channel function as interference to the modeling system. In order to avoid

the negative effects of the ECG components, the desired signal should be recorded when the ECG is absent, which is, however, impractical.

The period between the gradient pulses are filled with zeros. Due to these zeros, we can alleviate the abovementioned problems associated with the vector-sum reference signal.

To model the gradient source signal, we first detect the peaks of the MRGA in the vector sum. Later, the unit square pulses are generated synchronously with the detected peaks. The peaks of the MR gradient pulses are detected using an event detection processor. A block diagram of the event detection processor is shown in Fig. 4. This processor was implemented using the phase space method (PSM), which is a sort of a topology mapping method, and a least-squares acceleration filter (LSAF). The PSM is a topology mapping algorithm that can detect points from a characteristic form of the signal occurring in real time.[20] The PSM—a topology mapping method for peak detection—is advantageous in saving computational cost, which is important for real-time processing. Further, the LSA filter, a family of finite impulse response (FIR) filters, has been proposed to estimate the derivative or acceleration of a digitized signal.[9] LSAF is a simple mathematical algorithm used to detect the most morphologically distinct sharpness.[9]

Since the order of the LSA filter corresponds to the number of data points per window to be used in the sharpness estimates, we can simply adjust the order to make the window length equal to the typical duration of the waveform whose sharpness is to be measured. The output of a pth-order LSA filter, $\hat{x}(n)$, is defined as

$$\hat{x}(n) = \sum_{i=0}^{p-1} l_i \eta(n-i) \tag{17}$$

where $\eta(n)$ is the vector sum signal used as the input of the LSA filter and l_i, $0 \le i \le p-1$, are the weights of the LSA filter. This approach is (1) computationally simple, (2) can be performed in real time, and (3) is robust in the presence of noise. Furthermore, the design method is extended to derive FIR filters for estimating the derivatives of an arbitrary order in digital signals of biological or other origins.

In the course of the event detection process, the vector sum signal $\eta(n)$ is applied to the LSAF. After the LSA filtering, a topology mapping method is used to extract the peak points from the LSAF output. Finally, square pulses with a width W are generated synchronously to the detected peaks. The main steps in the synthesis of the reference input signal are as follows:

Step 1: A gradient-only signal can be synthesized through a vector sum (Eq. 16).
Step 2: To emphasize the peak of the MR gradient-only signal, the vector sum signal is applied to the LSAF (Eq. 17).
Step 3: A simple peak detection method based on the threshold and PSM is used to detect the peaks.
Step 4: Square pulses are synchronously generated to the detected peaks.

A synthesis example of impulse-like square pulses using an event detection processor is shown in Fig. 5. Figure 5a shows the three-lead ECG signals (Leads I, II, and III) corrupted by the gradient source in the MRI hardware amplifiers. Figure 5b shows the gradient-only signal $\eta(n)$ obtained by the vector sum, and Fig. 5c shows the output of the 5th-order LSA filter. The trajectories of the LSAF output signal are shown in Fig. 5e. The synthesized gradient-only signal and the LSAF output are mapped onto a two-dimensional phase space with respect to the delay of one sample corresponding to 1 ms. The region of the peak is shaded in the figures. In the phase space plot (Fig. 5e), peaks in the LSAF output signal of the vector sum signal appear in the third quadrant. Finally, synchronous impulse-like square pulses applied to the reference channel of the event-synchronous adaptive digital filter are generated. Figure 5f shows the synthesized impulse-like square pulses.

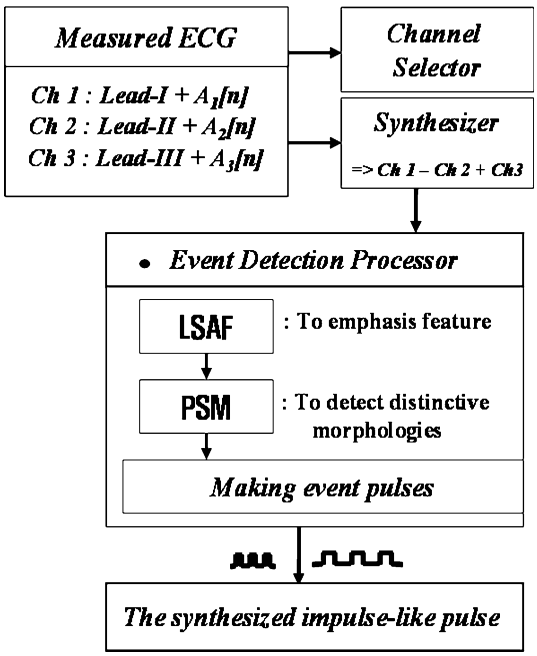

FIGURE 4. Block diagram of event detection processor.

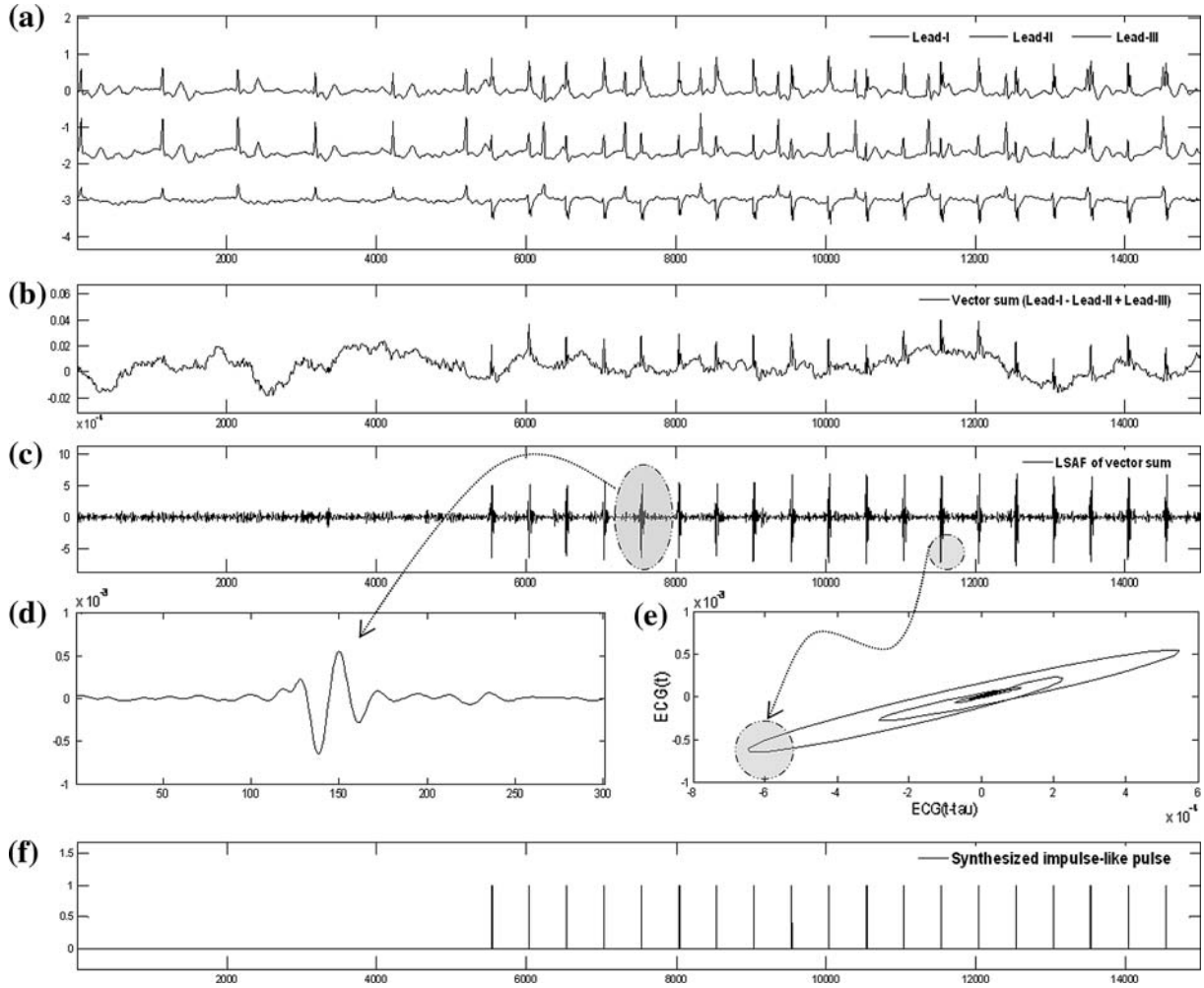

FIGURE 5. Synthesis of ES-AIC reference signal using vector sum of three-lead ECG and phase space plot of LSA-filtered output: (a) Three-lead ECG signal with MRGAs, (b) vector sum signal of three-lead ECG, (c) LSAF output of vector sum, (d) enlarged plot of grayed area, (e) phase space plot of (d), and (f) synthesized reference signal for ES-AIC.

Adaptive Estimation and Suppression of MRGAs

To address the time-varying feature of MRGAs in ECG leads, the adaptive estimation of MRGAs is necessary. For the updating process, the filter weights the adaptive algorithms. In this paper, we use a computationally efficient adaptive algorithm based on the least mean square (LMS) adaptive filter.

Laguna *et al.*[13] have proposed an ANC for the deterministic component of event-related signals that are time-locked to a stimulus, wherein a pulse related to the stimulus was used as a reference input. In this method, the deterministic component of the signal is estimated and the noise uncorrelated with the stimulus is removed, even if this noise is colored such as that in the case of evoked potentials; further, transient changes in the deterministic signal are better reflected than those obtained from an ensemble average method.[13]

The adaptive algorithm used in this study is a generalized form of a previous one described in Laguna *et al.*[13] In this study, the adaptive filter uses contaminated ECG signals $l_f(n)$ as the primary input. The reference signal $\hat{\mathbf{s}}(n)$ is a synthesized one comprising a sequence of unit square pulses with width W, instead of impulses. The square pulses are synchronized to the peaks of the MR artefacts in the ECG leads. As previously mentioned, the synthesized reference signal is used to model the MR gradient source signal $\mathbf{s}(n)$. By setting the inputs between the square pulses to zero, filter adaptation needs to be performed only during the period corresponding to the width of the square pulses. Thus, since the adaptation is synchronous to the detected events of the MRGAs, we will refer to this algorithm as the event-synchronous adaptive interference canceller (ES-AIC).

A schematic diagram of the proposed system is shown in Fig. 6. The weight vector of the adaptive filter is updated using the LMS algorithm. However, due to the special structure of the reference input, the

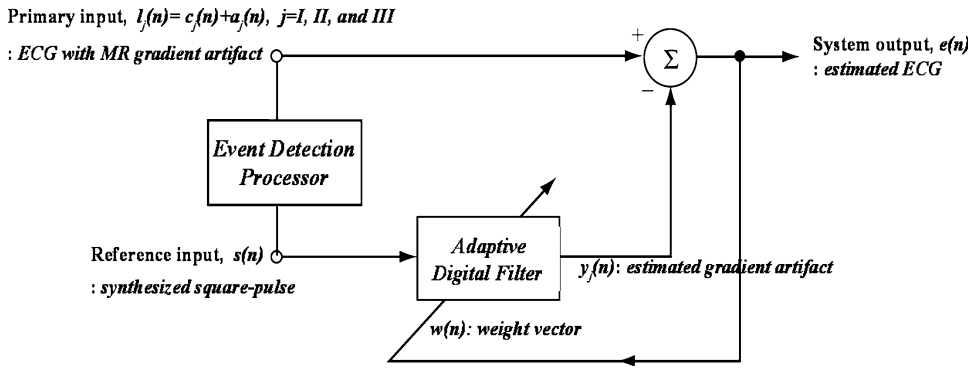

FIGURE 6. Schematic diagram of proposed system.

adaptive algorithm is reduced into a much simpler form than that in the conventional LMS algorithm. The reference input consists of unit square pulses of width W given by

$$\hat{s}(n) = \begin{cases} 1, & q_m \le n \le q_m + W - 1 \\ 0, & \text{otherwise} \end{cases} \tag{18}$$

where q_m is the location of the mth peak of the MR gradient.

Assume that the width of the square pulse W is much smaller than the filter order M. Since the reference input can have a value of either zero or one, the filter output $y(n)$ is computed as

$$y_j(n) = \bigcup_{q_m \in [n-M+1, n-W]} \left(\sum_{i=n-q_m-W}^{n-q_m} h_{j,i}(n) \right) \tag{19}$$

Now, the LMS algorithm for the weight update is summarized as

$$w_i(n+1) = \begin{cases} w_i(n) + \mu e(n), & n - q_m - W \le i \le n - q_m, \quad \text{for all } q_m \in [n-N+1, n-W] \\ w_i(n), & \text{otherwise} \end{cases} \tag{20}$$

where μ is the convergence parameter.

The proposed algorithm updates the weight vector only during the period corresponding to the width of the square pulses. Since the square pulses in the reference input are sparse, the filtering and update processes are performed over only a small portion of the input signal.

The advantages of this scheme are two-fold. First, we can minimize the effect of relatively strong interference, i.e., the ECG component, in the desired channel. In general, the weight vector can deviate from the optimal one if a strong interference is present in the desired channel.[11] Morphologically, the ECG component and MRGA are similar to each other.[1,7] Thus, it is desirable to minimize the amount of weight adjustment when the ECG component appears in the desired channel. Because of the zeros between the square pulses, the adaptive filter attempts to estimate only the components synchronized to the square pulses. In this way, the adaptive filter can minimize the effects of ECG components in the desired channel. In addition, the zeros minimize the effects of noise between the MR gradient pulses.

The second advantage of the proposed scheme is its computational simplicity. The filtering process described in Eq. (19) requires $W \times K$ additions, where K is the number of peaks of MRGAs within the time period covered by the M-sample reference input. The LMS update procedure described in Eq. (20) also requires $W \times K$ multiply-and-accumulate (MAC) operations.

The proposed algorithm requires an on-line event detector and adaptive filter working on a sample-by-sample basis and it does not introduce any algorithmic bulk-delay. One possible delay is the one caused by input-output buffering of the real-time system. The essential adaptation time, which is feature of early state at application of adaptive filter, is appeared as another delay unit which needs a few periods of ECG. There is a data I/O unit with FIFO (First Input First Output) structure which is used as input-out buffering in data acquisition system. However, the delay of the real-time I/O depends on the hardware, which is beyond the scope of this paper. The real-time I/O implemented on the test system is designed by the embedded system with a ADC and DSP (Digital Signal Processor).

EXPERIMENTAL SETUP

Experimental Details

The experiments were conducted on a 0.35 T MRI system. The ECG data were collated using preamplifiers and analog band-pass filters with four carbon electrodes and a sampling rate of 10 kHz. The preamplifier gain was 1000 (60 dB), and the bandwidth of the analog filter was 0.1–500 Hz. The data acquisition system was located in a shielded box. The carbon electrode leads (coax cables, 1 mm thick, and 200 cm long) were bundled together and firmly fixed. Precaution was taken not to put any loops in the leads. Next, the leads were attached to the inputs of the ECG preamplifier just outside the magnet's bore. The amplified signal was then carried through a current loop drive to the PC. A block diagram of the measurement system is shown in Fig. 7. Simultaneous ECG/MRI acquisition was performed using normal subjects, and the tested arrangement of the electrode position is shown in Fig. 8. Various imaging sequences, such as spin echo (SE), fast spin echo (FSE), gradient echo (GE), and fast gradient echo (FGE) were applied with various echoes (TE), repetition times (TR), and number of image slices. The recording for each sequence was performed for 2–5 min.

Performance Metric for MRGA Suppression

In this section, the efficiency and accuracy of the method were demonstrated by post-processing a large number of ECG signals from a widely different set of MR pulse sequences and also by performing real-time tests on adult subjects under standard MRI scanning conditions.

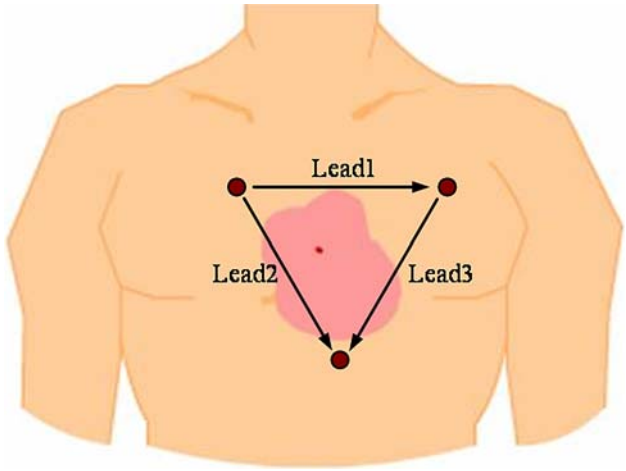

FIGURE 8. Tested electrode position.

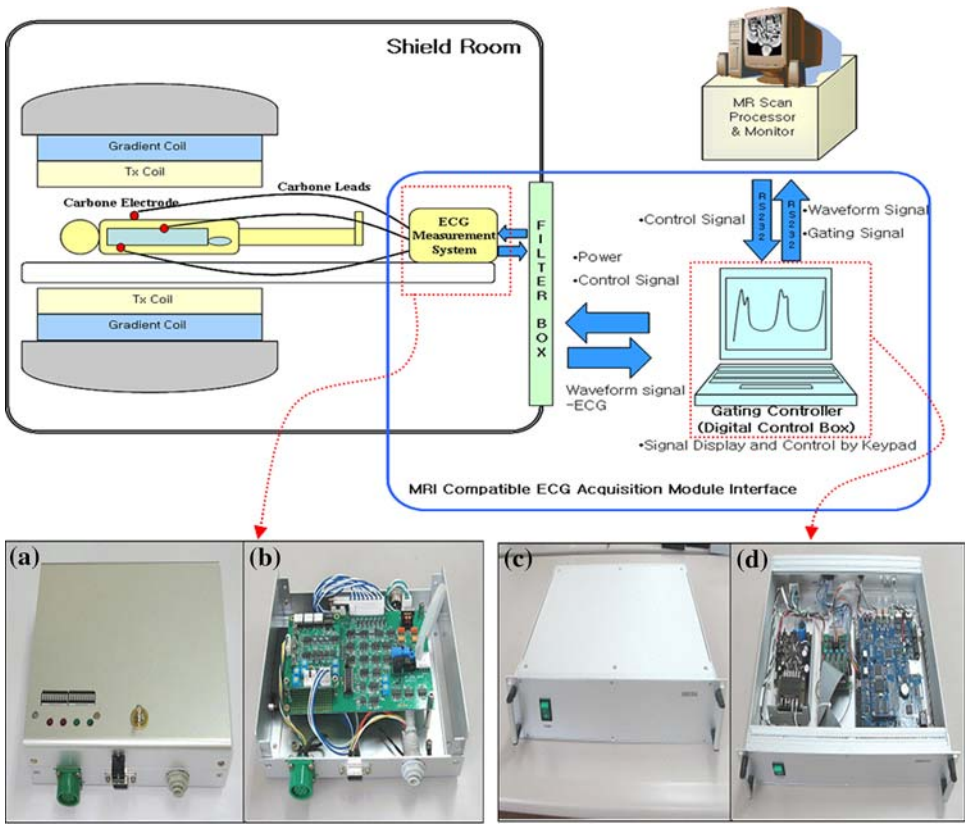

FIGURE 7. Block diagram of measurement system: (a, b) ECG measurement system; (c, d) gating controller (digital control box).

We analyzed the MR interference induced during various gradient scenarios. Further, we evaluated the performance of the proposed method using various types of simulated and real data sets. The proposed method was compared with a multichannel ANC, which was previously proposed in Abacherli *et al.*[1] where a more general method in adaptive estimation was employed. In order to determine the performance, we measured the signal-to-noise ratio (SNR) improvement defined as

$$\mathrm{SNR}_d = \frac{E[c_k^2]}{E[a_k^2]} = \frac{E[c_k^2]}{E[(l_k - y_k)^2]}. \qquad (21)$$

where $E[c_k^2]$ and $E[a_k^2]$ are the expected values of c_k and a_k at a discrete time k and y_k is the filter output. In our setup, c_k denotes the ECG; a_k, MRGA; and l_k, the sum of the ECG and artefact. In our setup, SNR implies the power ratio of the ECG and MRGA. The objective of the performance metric is to determine SNR enhancement between the input signal l_k and filter output signal y_k, which is correlated with c_k.

When the algorithm has converged to the steady state, the SNR was calculated using c_k, a_k, and y_k. Further, we repeated the simulation using different noise sequences and the same ECG signal. In this study, we used the LMS algorithm to adjust the weights in our adaptive process. The order of the filter was 180, and a learning rate was experimentally set to 0.1.

RESULTS

ECG–MRGA Shape Analysis and Synthesis of Reference Signal

When a strong magnetic field was radiated by the gradient coil, MRGAs induced on the ECG trace considerably depended on the gradient scenarios. In this section, the MRGAs on the ECG signals for the various scenarios were analyzed. Figure 9 shows an analysis of the MRGAs on ECG signals during specific gradient scenarios, namely, SE with a TR value of 200 ms.

The first panel of Fig. 9 shows the gradient waveforms in three diffusion directions (x, y, and z). The second panel shows Leads I, II, and III of the ECG. The third panel shows the signal synthesized as the vector sum of the three ECG leads, which was used to formulate the reference signal of the ES-AIC. The last panel shows the time-frequency analysis of the synthesized signal (the third panel). In the ECG, the vector sum defined as "Lead I − Lead II + Lead III" leads to a characteristic function with a zero value. To analyze this characteristic feature, we used the time-frequency analysis: when considering a signal that is a mixture of ECG and MRGAs, this method is a very effective way to determine the spectral density of each signal. In particular, it is a much more effective method in examining the energy distribution of a signal, including a heavy peak, for a specific time. As can be

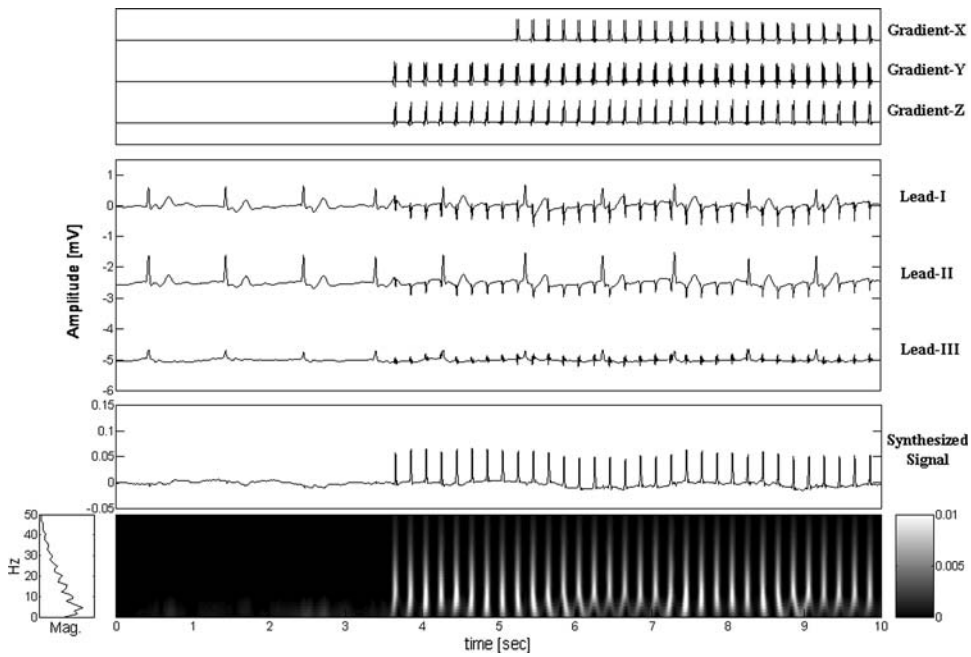

FIGURE 9. MR interference analysis during SE scenarios of gradient. The first panel shows the gradient waveforms in three diffusion directions (*x*, *y*, and *z*). The second panel shows Leads I, II, and III of the contaminated ECG. The third panel shows the signal synthesized as the vector sum of the contaminated three ECG leads. The last panel shows the time-frequency analysis of the synthesized signal which is shown in the third panel.

seen from the time-frequency analyses (the last panel), the synthesized reference signal obtained from the vector sum does not contain the ECG components, as shown in Fig. 9. Therefore, the synthesized reference signal can be efficiently used to develop the reference signal of the ES-AIC, as shown in Fig. 5.

Simulation Study

A simulation study was carried out to test the performance of the proposed method. To quantitatively evaluate if the proposed filter sufficiently eliminates MRGAs induced in the ECG, both the ECG and the artefact signal applied to the input node of the proposed filter should be necessarily known. Further, the performance of the proposed filter can be estimated more objectively by using the simulated data than the actual patient data. Pure MRGA and a pure ECG signal is necessary to accurately evaluate the performance. Therefore, we used an artificial experiment to simulate our setup. To generate various simulation data sets according to the MR gradient scenarios, we used various simulation setups.

A test signal was synthesized as a sequence of records d_k. Each one consisted of a pure ECG signal (c_k), taken from a real ECG signal, and additive MRGA (a_k). Attaching ECG electrodes to the lower right arm enabled the acquisition of pure MRGA because ECG could not be measured in this position. Further, a pure ECG signal could be measured easily in the gradient-off condition. Through the linear summation of pure MRGAs and pure ECG signal, the simulation signals (l_k) were formulated.

Figure 10 shows the time courses of the simulation data for a SNR value of −3 dB in the case of SE, FSE, GE, DW-EPI scenarios, which are the various simulation data.

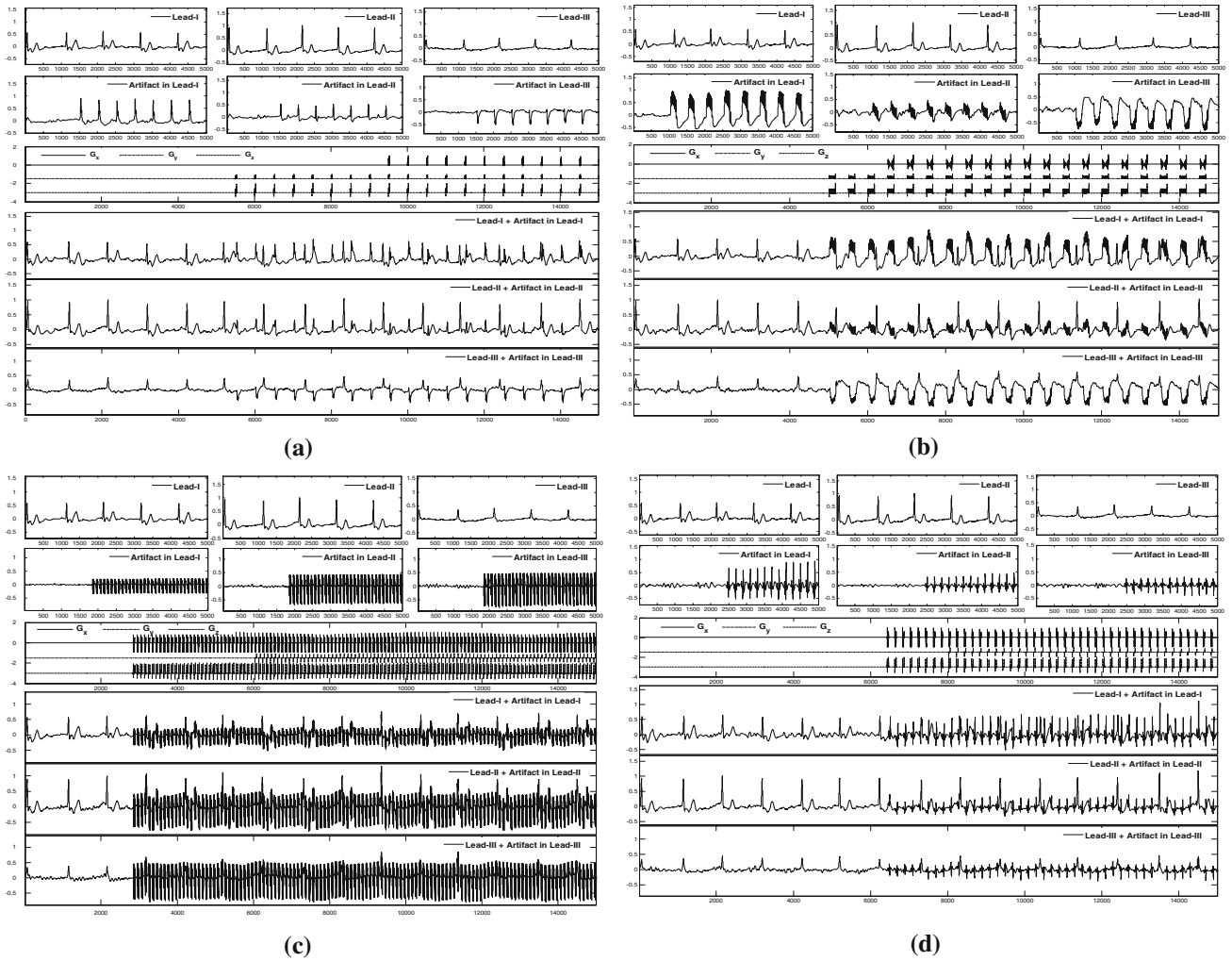

FIGURE 10. Simulated data set through linear summation of pure MRGAs and pure ECG signal: (a) SE, (b) FSE, (c) GE, and (d) DW-EPI scenarios.

At the top, we can see pure ECG signals (Leads I, II, and III), which are present in each lead. The second row displays three-lead MRGAs induced in the human body. The third row shows the output signals of the three gradient amplifiers (G_x, G_y, and G_z) in the MRI hardware system. Next, the three-lead ECG signals with MRGAs, which were used as the input of the ES-AIC, are shown in the last three rows after a linear summation of the ECG and artefacts. The signal resolution was 16 bit, and it was sampled at 1 kHz.

We analyzed various simulation data which are shown in Fig. 10. Further, the proposed ES-AIC and ANC with a multichannel reference were compared. Both the above mentioned filters were applied to the simulation signal d_k. Moreover, a reference signal for the proposed ES-AIC was synthesized as an impulse-like pulse at the beginning of an incoming gradient and three reference signals (G_x, G_y, and G_z) for the ANC with a multichannel reference were acquired in the gradient amplifier of MRI.

In addition, the various SNR values were studied by changing the power of the ECG signal because the performance of the filter can be different according to the relative power of the artefact and ECG signal. Further, many different gradients in various scenarios were applied. For each scenario, the signals with a SNR value of 30 dB are generated by increasing the SNR value from −20 dB to 10 dB for an increment rate of 1 dB. After applying the simulation data to the proposed method, the mean square error (MSE) of the estimated ECG and SNR improvement were calculated. Figure 11 shows several results obtained using the proposed ES-AIC and multichannel ANC according to the simulation data with different SNR values.

In this analysis, the proposed ES-AIC and multichannel ANC yielded comparable results; therefore, we can verify the filter performance under the simulation conditions. The top row shows a pure ECG signal, and the second, third, fourth, and fifth rows list the results using two filtering methods according to the data with different SNR values. Here, we can see that the ES-AIC performs as effectively as the multichannel ANC, but the results in Fig. 11 are not sufficiently distinguishable to quantitatively evaluate the performance.

Therefore, we quantitatively analyzed the performance using a MSE curve according to the SNR value. Figure 12 shows the MSE according to the variation in the SNR values of the simulated data. Figure 12 shows a comparison of the performance for different noise levels. The parameters of all the scenarios are the same as those above. Here, the learning rate of the two methods is set to 0.01.

Cancellation of MRGAs Using Real Data

Based on the abovementioned results, the performance of the filter using real data was evaluated. Figure 13 shows the results for three types of real data

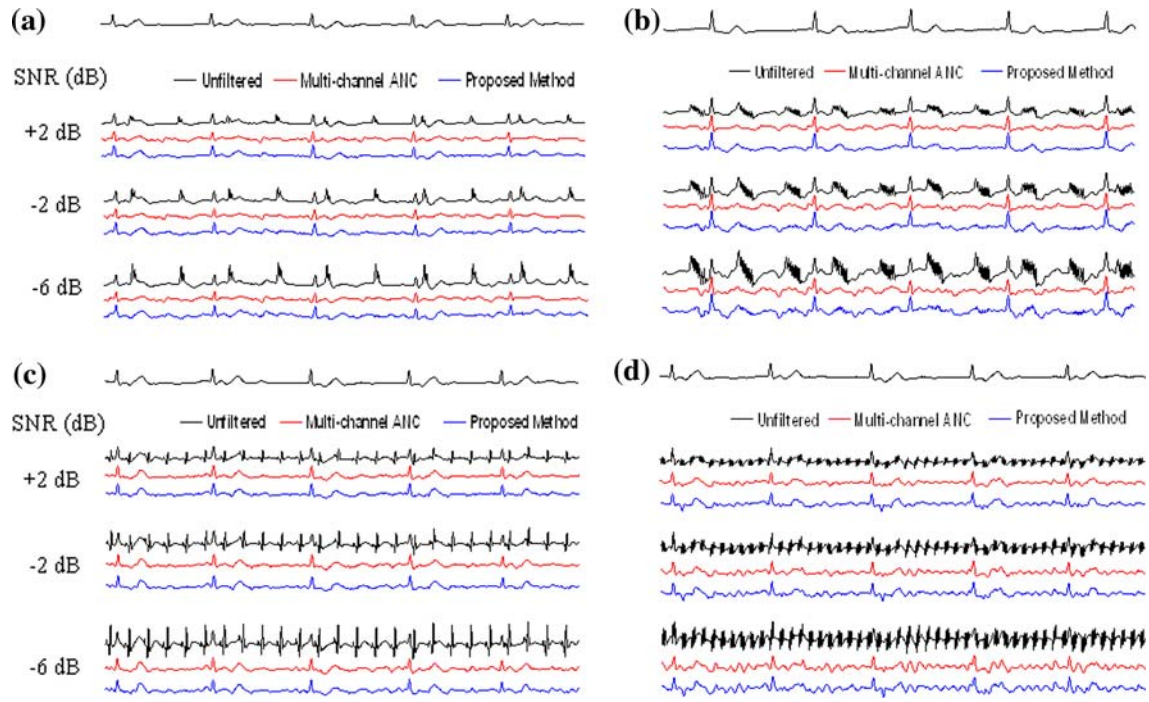

FIGURE 11. Simulation results according to data obtained using various SNR values: (a) SE, (b) FSE, (c) GE, and (d) DW-EPI scenarios.

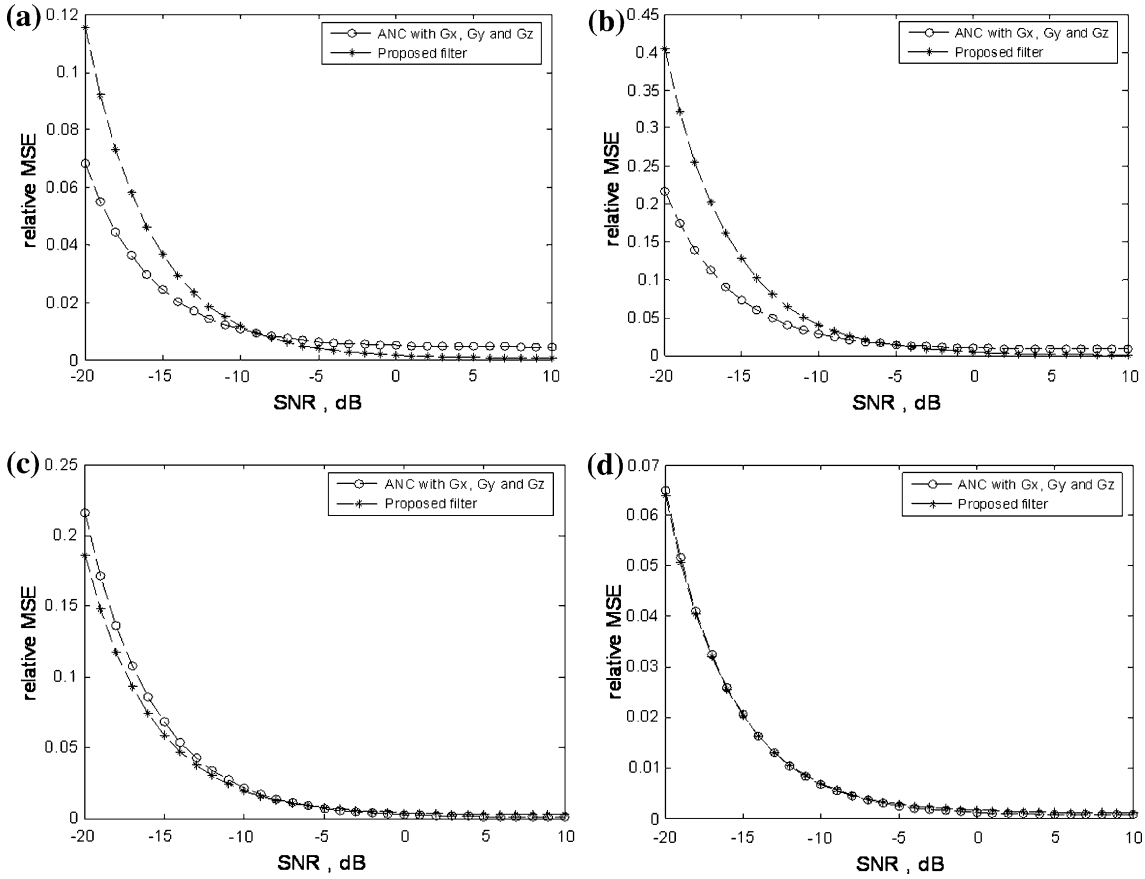

FIGURE 12. MSE obtained by the variation in SNR of simulated data: (a) SE, (b) FSE, (c) GE, and (d) DW-EPI scenarios.

measured from the subjects. Three types of real data are GE, DW-EPI and SE scenarios. Especially the real data of the SE scenario was measured using high-power gradient source for the experiment with the worse SNR. The first row of Fig. 13 shows the ECG signal disturbed by the MRGAs. The second row shows the output signal obtained after filtering by the proposed method, and the bottom row shows the finally generated gating-pulse signal. Through these examples shown in Fig. 13, the MRGAs induced in the ECG lead were successfully estimated and cancelled at the output of the ES-AIC. Further, similar results were obtained for the sets of scenarios with different gradients. The initial adaptation time, which is an essential measurement for the evaluation of the adaptive filter, is represented in the shaded area shown in Fig. 13. However, a little convergence time is not important for the cardiac gating application because additional time for a dummy scan can exist in the case of image scanning. In the figures, the locations of the QRS complexes are evident. It can be seen that even though MRGAs are still visible, an accurate generation of the MR gating pulse by using the proposed method was possible.

Improvements in MR Image Using Proposed Cardiac Gating Method

The global evaluation of the algorithm was done in terms of image quality. The image, acquired with synchronization, revealed a very clear enhancement as compared to the cardiac MRI taken without cardiac gating. This result is shown in Fig. 14. Further, we performed the cardiac phase imaging according to a trigger delay using MR gating pulses. Figure 15 shows the result of such cardiac phase imaging. From the abovementioned results, clearer structures could be observed in the image close to the heart when the cardiac gating technique was employed. Furthermore, we observed a better contrast in the entire image, and the structures were more emphasized.

DISCUSSION

The adaptive digital filter has been considered to be an effective method for reducing MRGAs. In a previous method that used adaptive digital filters,[1] the three gradient currents were required to be determined either by a direct connection with the MR system or by using

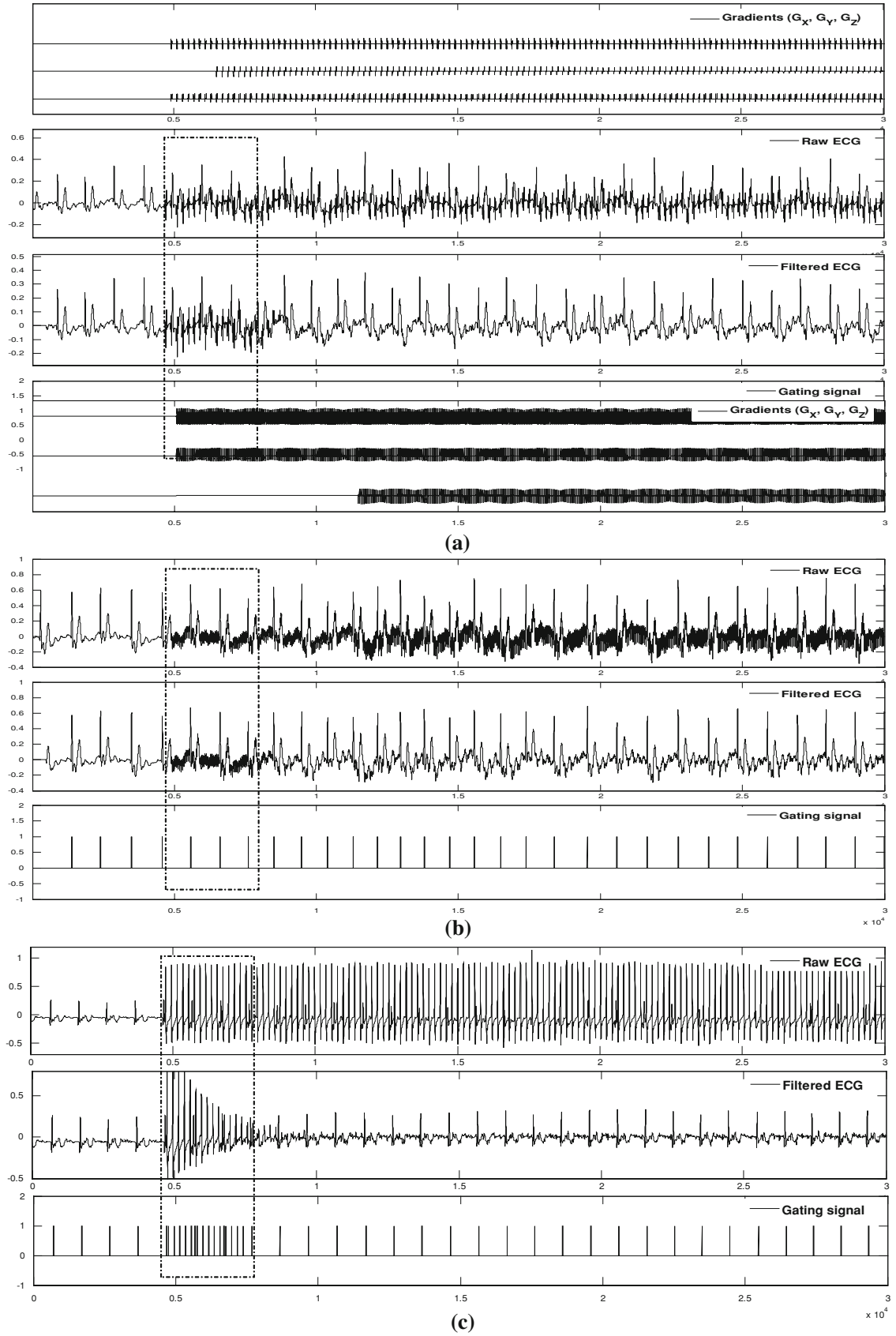

FIGURE 13. Results for real data according to various MR imaging scenarios: (a) GE, (b) DW-EPI, and (c) SE scenarios.

three-dimensional pick-up coils. The linearity of the four signals used (ECG, G_x, G_y, and G_z) is essential for the assessment of the system response and the restoration process, and the sampling rate should be sufficiently high to accurately acquire the gradient shapes.

Therefore, we used a new adaptive ES-AIC based on an impulse-like reference signal that is synthesized synchronously to the MRI gradient signal induced in the ECG leads: here, impulse-like pulse signals were used as a reference signal to the ES-AIC. By using the proposed ES-AIC, we could reduce the computational complexity in real-time processing. Furthermore, the extracted reference signal is independent of the MRI machine. Therefore the proposed method can be implemented without additional hardware. Further, unlike "combined wavelet sub-band decomposition and adaptive filtering,"[2] the proposed filter does not require a training MRI scan and accompanying ECG signal acquisition to compute an estimate of the impulse response matrix.

Our goal was a development of cardiac gating system for conventional 0.35 T permanent type MRI.

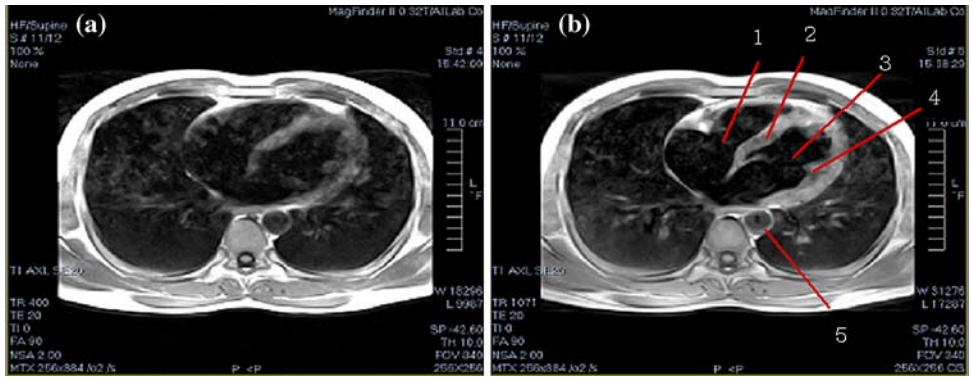

FIGURE 14. Cardiac image enhancement with cardiac gating: (a) No ECG gating; (b) ECG gating; (1) right ventricle, (2) interventricular septum, (3) left ventricle, (4) papillary muscle, and (5) descending aorta.

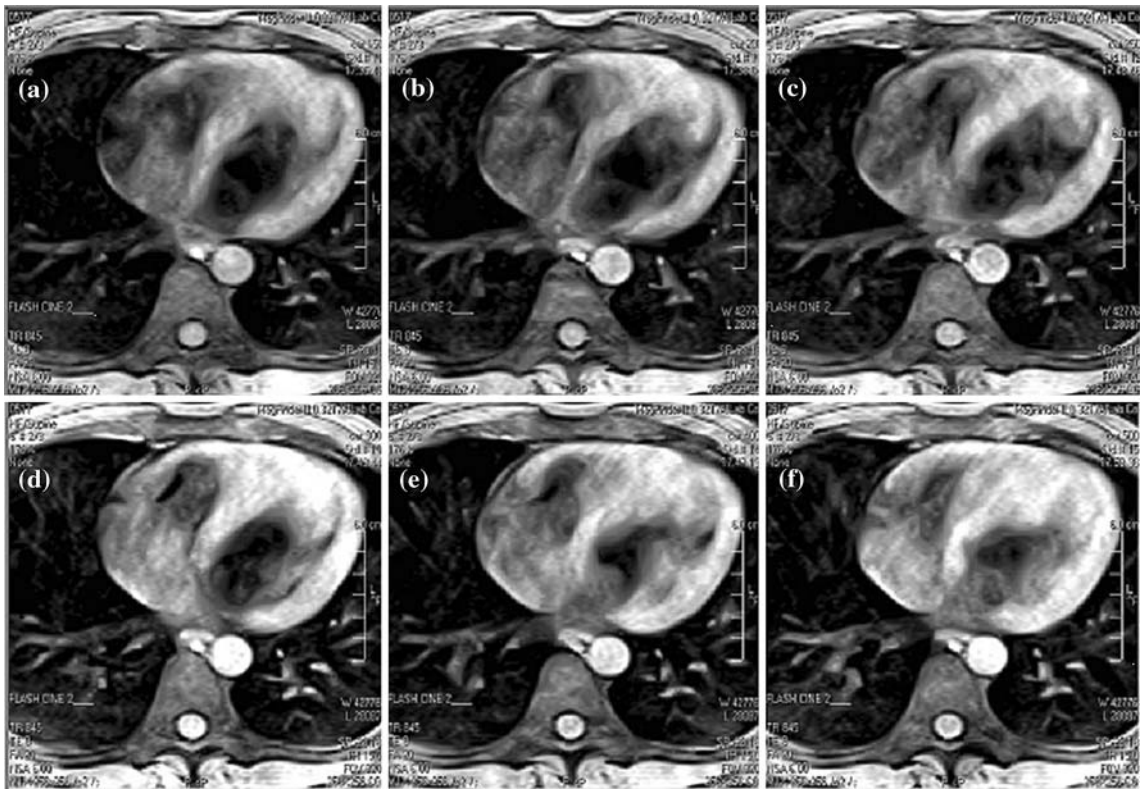

FIGURE 15. Cardiac phase images according to trigger delay: Trigger delays of (a) 150 ms, (b) 200 ms, (c) 250 ms, (d) 300 ms, (e) 400 ms, and (f) 500 ms.

Recently in general clinical environment an over 1.5 T super conduct MRI is being used. However the experiments in this paper have been conducted on the limited condition, a 0.35 T permanent type MRI, not an over 1.5 T super conduct type MRI. The higher is the field intensity, the more serious is the artefacts. Moreover, MRGAs are due to the temporal variations of the magnetic field gradients. We can generally say that the corresponding induced voltages are influenced mainly by switching of magnetic field gradient, rather than static magnetic field. Therefore, we can think that the morphology pattern of the MRGAs in the high field intensity is similar to that in the low field intensity. Also the proposed methodology in a clinical environment is thought to be used well.

In our proposed ES-AIC, the following detailed remarks can be discussed.

Synthesis of Reference Input Signal in Proposed ES-AIC

The ES-AIC uses a square event-pulse signal, which is synchronous to the gradient pulses of the MRI, as a reference signal event. The square pulses that are synchronously generated in the event detection process were applied to the reference channel of the ES-AIC.

The direct extraction of the reference signal from the three-lead ECG signal contaminated by MRGAs was very important. As shown in Fig. 5, our proposed method of generating the reference signal showed a good performance and worked perfectly.

Instead of the proposed event detection process, an event-detector-based "combined wavelet sub-band decomposition" used in Abi-Abdallah *et al.*[2] can be considered.

In the proposed event detection process, the synthesis course of the event pulses was very simplistic for implementation because the LSAF and PSM used in the event detection process shown in Fig. 4 were simple mathematical algorithms. Furthermore, an additional advantage of our method was that no external devices for acquiring the gradient pulse signals were required.

The origin of the abovementioned advantages is as follows: a vector sum defined by "Lead I − Lead II + Lead III" leads to a characteristic function with a zero value in the ECG signal, but the MRGAs in the three leads are not cancelled by the vector sum. The vector sum only includes the artefacts induced by the MR gradients.

Proposed ES-AIC for Minimizing MRGAs

In the adaptive filter theory, it is known that the interference in the desired channel can affect the performance of the adaptive filter. Since the ECG signal component in the desired signal can be relatively strong in terms of the SNR, the adaptive filter is likely to be interfered by the presence of the ECG signal component in the desired input. Moreover, the ECG signal is highly correlated with the gradient signal in the reference channel; in order to obtain accurate estimates, the ADF order should be sufficiently large to include the period of the MRI gradient signal. For example, a 200-ms MRI scan will generate MRGAs with a period of 200 samples when the signals are sampled at 1 kHz. In this case, the desirable ADF order would be 200, which may be computationally too complex for real-time processing.

By using a new adaptive ES-AIC based on an impulse-like reference signal that is synchronously synthesized to the MR gradient signal induced in the ECG leads, we have reduced the computational complexity. In order to optimally estimate the MRGA response, the operation of the ES-AIC was based on a scaling reference signal. When applying variations only to the amplitude of the MRGA, a scaling of the reference signal is needed to generate a perfect match of the present frame. If a cross-correlation exists between the ECG of the present frame and the MRGA of the reference signal, the adaptive filters might also adapt to this correlation. In this case, the filter will attempt to not only eliminate the MRGA but also parts of ECG where the correlation exits. To avoid this effect, the ECG and MRGA of the frames under consideration should be mutually uncorrelated. The component correlated with the ECG will be shown as a remainder artefact. In our case, the ECG within a frame can be a correlated signal. In a practical system, this effect must be considered because it causes a reduction in the ECG power.

In short, by considering a small calculation power, the ES-AIC algorithm can be applied to the real-time removal of MRGAs.

Comparisons of Multichannel ANC and Proposed ES-AIC

Comparing the results in Fig. 12, the similarity in the performances of the ES-AIC and multichannel ANC is evident. However, it is found that the convergence rates of the multichannel ANC are generally better. However, the convergence rate of the ANC is significantly influenced by the noise level. In Fig. 12, it can be clearly seen that multichannel ANC has a better performance in the low-SNR region (below −10 dB), but the ES-AIC has a better performance for SNR values above −10 dB. In this process, we used the LMS algorithm to update the coefficients for the proposed ES-AIC, but we used the normalized least mean square (NLMS) algorithm to update the coefficients of the multichannel ANC.

On the basis of the data obtained from the subjects, the proposed ES-AIC showed a very promising performance. This method was capable of effectively eliminating most of the MRGAs with only occasional artefacts remaining in the output signal. Even though the MRGAs can be considerably reduced in the ECG signal by the use of the proposed method, very trivial distortion still appears in the ECG signal.

Nevertheless, reliable gating can reduce false-positive triggers and increase image quality. The proposed method reduces the filter delay for calculating the system response.

From the abovementioned results, we found that the multichannel ANC is slightly superior to the ES-AIC. However, the ES-AIC had a better calculation performance than the multichannel ANC.

CONCLUSION

We have proposed an "event-synchronous adaptive interference canceller (ES-AIC)," a gradient-wise reduction filter, which is simple but effective. The filter restores the ECG signals contaminated by MRGAs acquired during MR sequences. The LMS algorithm was used for updating the ES-AIC coefficients. In particular, the proposed ES-AIC does not require reference signals from an MR scanner. The reference signals of the ES-AIC used in this study were obtained using a combination of noisy three-lead ECG signals.

The ES-AIC performance was measured off-line, and a gating pulse was generated using point-by-point operations. The quality of the filtered ECG was so reliable that the QRS detector could be used to correct the triggering/gating of the MR machine. Our results conclusively show that the ES-AIC is applicable even when the scenario of the MR sequence in the magnet bore is changed.

In particular, the proposed method was based on a simple experimental setup and did not require any physical connections from the gradient amplifiers of the MRI machine. The proposed method can also be used in MR imaging with the application of real-time implementation because it is very efficient in calculation. In order to finally determine the efficiency of the proposed method, the filter should be tested on a larger population of individuals.

As applications of the proposed system, reliable cardiac monitoring information can be provided to the physician and the ES-AIC in the MR gating method using other physiological signals can be made possible.

ACKNOWLEDGMENT

This study was supported by a grant from the Industrial Cluster Policy, Ministry of Knowledge Economy, Republic of Korea.

REFERENCES

[1]Abacherli, R., C. Pasquier, F. Odille, M. Kraemer, J.-J. Schmid, and J. Felblinger. Suppression of MR gradient artefacts on electrophysiological signals based on an adaptive real-time filter with LMS coefficient updates. *MAGMA* 18:41–50, 2005.

[2]Abi-Abdallah, D., A. S. Drochon, V. Robin, and O. Fokapu. Cardiac and respiratory MRI gating using combined wavelet sub-band decomposition and adaptive filtering. *Ann. Biomed. Eng*. 35(5):733–743, 2007.

[3]Allen, P. J., O. Josephs, and R. Turner. A method for removing imaging artefact from continuous EEG recorded during functional MRI. *Neuroimage* 12:230–239, 2000.

[4]Bonmassar, G., P. L. Purdon, I. P. Jaaskelainen, K. Chiappa, V. Solo, E. N. Brown, and J. W. Belliveau. Motion and ballistocardiogram artefact removal for interleaved recording of EEG and EPs during MRI. *Neuroimage* 16:1127–1141, 2002.

[5]Damji, A. A., R. E. Snyder, D. C. Ellinger, F. X. Witkowki, and P. S. Allen. RF interference suppression in a cardiac synchronization system operating in a high magnetic field NMR imaging system. *Magn. Reson. Imaging* 6:637–640, 1988.

[6]Dimick, R., L. Hedlung, R. Herfkens, E. Fram, and J. Utz. Optimizing electrocardiograph electrode placement for cardiac gated MRI. *Invest. Radiol*. 22:17–22, 1987.

[7]Felblinger, J., J. Slotboom, B. Kreis, B. Jung, and C. Boesch. Restoration of electrophysiological signal distorted by inductive effects of magnetic field gradients during MRI sequences. *Magn. Reson. Med*. 41:715–721, 1999.

[8]Fischer, S. E., S. A. Wickline, and C. H. Lorenz. Novel real-time R-wave detection algorithm based on the vectorcardiogram for accurate gated magnetic resonance acquisitions. *Magn. Reson. Med*. 42:361–370, 1999.

[9]Frei, M. G., R. L. Davidchack, and I. Osorio. Least squares acceleration filtering for the estimation of signal derivatives and sharpness at extrema. *IEEE Trans. Biomed. Eng*. 46(8):971–977, 1999.

[10]Goldman, R. I., J. M. Stern, J. Engel, and M. S. Coen. Acquiring simultaneous ECG and functional MRI. *Clin. Neurophysiol*. 111:1974–1980, 2000.

[11]Haykin, S. Adaptive Filter Theory. New Jersey: Prentice-Hall, 2002.

[12]Kerger, K. S., and C. R. Giordano. Biopotential adaptive filtering in an MR environment. In: Proceedings of the SMRM 12th Annual Meeting, Berlin, p. 661, 1992.

[13]Laguna, P., R. Jane, O. Meste, P. W. Poon, P. Caminal, H. Rix, and N. V. Thakor. Adaptive filter for event-related bioelectric signals using an impulse correlated reference input: comparison with signal averaging techniques. *IEEE Trans. Biomed. Eng*. 39(10):1032–1044, 1992.

[14]Larson, G., R. D. White, G. Laub, E. R. McVeigh, D. Li, and O. P. Simonetti. Self-gated cardiac cine MRI. *Magn. Reson. Med*. 51:93–102, 2004.

[15]Laudon, M. K., J. G. Webster, R. Frayne, and T. M. Grist. Minimizing interference from magnetic resonance imagers during electrocardiography. *IEEE Trans. Biomed. Eng.* 45(2):160–164, 1998.

[16]Moore, J. Method of improving the quality of an ECG obtained from a patient undergoing magnetic resonance imaging. US Patent 4991580, 1991.

[17]Rokey, R., R. Wendt, and D. Johnston. Monitoring of acutely ill patients during nuclear magnetic resonance imaging, use of a time varying filter ECG gating device to reduce gradients artefacts. *Magn. Reson. Med.* 6:240–245, 1985.

[18]Shetty, A. N. Suppression of RF interference in cardiac gated MRI: a simple design. *Magn. Reson. Med.* 8:84–88, 1988.

[19]Sijbers, J., I. Michiels, M. Verhoye, J. van Audekerke, A. van der Linde, and D. van Dyck. Restoration of MR-induced artefacts in simultaneously recorded MR/EEG data. *Magn. Reson. Med.* 17:1383–1391, 1999.

[20]Srinivasan, N., M. T. Wong, and S. M. Krishnan. A new phase space analysis algorithm for cardiac arrhythmia detection. *EMBC* 82–85, 2003.

[21]Van Genderingen, H. R., M. Sprenger, J. W. de Ridder, and A. C. van Rossum. Carbon fiber electrodes and leads electrocardiography during MR imaging. *Radiology* 171:872, 1989.

[22]Wendt, R. E., R. Rockey, G. W. Vick, and A. L. Johnston. Electrocardiographic gating and monitoring in NMR imaging. *Magn. Reson. Imaging* 6:89–95, 1988.